

## Full Paper

**Evaluation of (S)- and (R)-Misonidazole as GPX Inhibitors: Synthesis, Characterization Including Circular Dichroism and *In Vitro* Testing on Bovine GPx-1****Felix Wilde, Chamseddin Chamseddin, Heidi Lemmerhirt, Patrick J. Bednarski, Thomas Jira, and Andreas Link**

Department of Pharmaceutical and Medicinal Chemistry, Institute of Pharmacy, Ernst-Moritz-Arndt University Greifswald, Greifswald, Germany

Racemic misonidazole, a radiosensitizer formally used in radiation therapy of cancer and to date still applied, was once reported to exhibit strong inhibitory effects on mouse glutathione peroxidases (GPX). This appeared to qualify misonidazole as a lead structure for the development of novel GPX inhibitors to cause oxidative stress in chemotherapy-resistant tumors. A unique feature of misonidazole as an inhibitor of GPX is the absence of a thiol functionality. Therefore, it was expected to selectively target inhibition devoid of promiscuous interactions with cations and sulfhydryl groups. We synthesized the isomers of misonidazole and analyzed the ability of chiroptical high-performance liquid chromatography (HPLC) to identify the particular enantiomers. Due to the chiral pool synthesis, the assignment of the correct configuration could be verified. Finally, we evaluated both isomers for their inhibitory activities on bovine erythrocyte GPx-1, which is 87% homologous to the human enzyme. Despite the previously reported inhibition of racemic misonidazole on the less homologous mouse GPx-1, we did not find any significant inhibitory activity on the bovine enzyme for either isomer. Though misonidazole appears unlikely to be an inhibitor of human GPx-1 activity, we still spotlight misonidazole as a promising fragment-like lead structure in general.

**Keywords:** Circular dichroism / Glutathione peroxidase / *In vitro* inhibition / Lead structure / Misonidazole

Received: August 1, 2013; Revised: September 24, 2013; Accepted: September 24, 2013

DOI 10.1002/ardp.201300285

**Introduction**

Racemic misonidazole was developed as one of the first nitroimidazoles used as a radiosensitizer [1], but it showed dose-limiting neurotoxicity and overall poor results in clinical trials [2]. The idea of generating nitro radicals in hypoxic tissue to bring about covalent binding to the DNA was confirmed [3]. The absence of oxygen also leads to an accumulation of the drug, making it one of the most extensively explored radiotracers for hypoxia in tissues [4]. Recently it was even reported to be a promising tool for the detection of hypoxia in micrometastases, which might help to delimit malign tumors from noncancerous diseases, like lung

nodules [5]. Kumar and Weiss [6] reported that misonidazole also has potent inhibitory activity against glutathione peroxidase (GPX) from mouse liver. GPX, the first selenocysteine enzyme described [7], metabolizes H<sub>2</sub>O<sub>2</sub> and organic peroxides to water and alcohols, respectively. To survive redox stress incurring from permanent proliferation, cancer cells often raise their levels of GPX [8]. Thus, GPX inhibitors might offer a novel therapy to treat cancer, especially after they have become resistant to chemotherapy [9]. Most of the known inhibitors of GPX, however, contain a thiol functionality, which is easily oxidized and complexes readily with ubiquitous metal ions, thus making such compounds poor drug candidates. Non-thiol substances such as misonidazole would appear interesting starting points for the development of novel GPX inhibitors. Thus, we were interested in re-evaluating the GPX inhibitory activity of misonidazole on bovine GPx-1, which has a closer homology to the human enzyme than mouse GPx-1. Here we present the synthesis and

**Correspondence:** Prof. Andreas Link, Department of Pharmaceutical and Medicinal Chemistry, Institute of Pharmacy, Ernst-Moritz-Arndt University Greifswald, 17487 Greifswald, Germany.

**E-mail:** link@pharmazie.uni-greifswald.de**Fax:** +49 3834 864802

characterization of the misonidazole enantiomers as well as their ability to inhibit bovine GPx-1.

## Results

### Synthesis of misonidazole enantiomers

The synthesis of 2-aminoimidazole (**3**) as hemisulfate salt was performed in analogy to a previously reported procedure [10]. Accordingly, 2-aminoacetaldehyde dimethyl acetal **2** was added to *O*-methylisourea sulfate **1** under an argon atmosphere. The reaction mixture was adjusted to pH of 2–3 by means of concentrated sulfuric acid, giving a brownish mixture that further darkened upon stirring at elevated temperature. After work-up, the hemisulfate salt **3** was obtained as light brown crystals in good yields (Scheme 1).

The synthesis of 2-nitroimidazole (**4**) was based on the procedure reported by Yang and Goldberg [11]. Dilute sulfuric acid was cooled to 0°C; then copper sulfate and hemisulfate **3** were added slowly to prevent the reaction temperature from rising above 20°C. The resulting green solution was cooled to –20°C under vigorous stirring. During the careful addition of an aqueous solution of sodium nitrite, brown gas evolved and the color turned dark blue. The reaction mixture was allowed to stand at room temperature for 1 week to give a green solution with some white precipitate. While keeping the temperature below –8°C, NH<sub>3</sub> gas was slowly bubbled through the solution until it was adjusted to pH 1. Afterwards the reaction mixture was stirred for another 3 h at 0°C. The yield of the yellow precipitate of **4** was insufficient. Therefore, the product containing reaction mixture was worked up by extraction. The combined precipitated and extracted product fractions together gave a small but sufficient amount of yellow 2-nitroimidazole (**4**) for the subsequent alkylations with enantiomerically pure 2-(methoxymethyl)oxiranes **5** (Scheme 2).

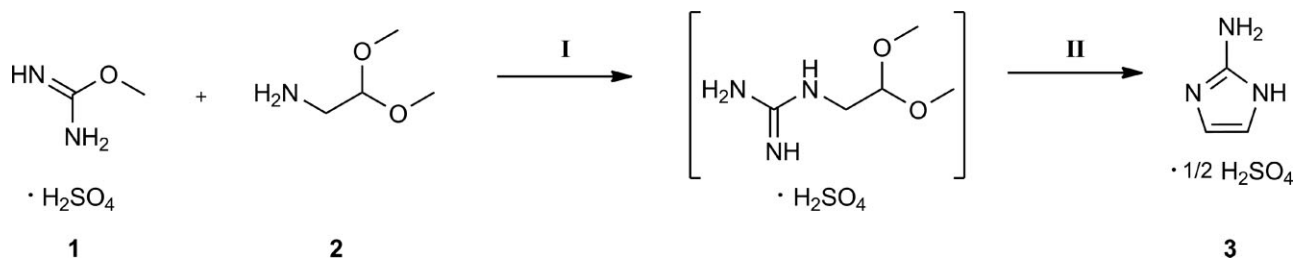
The synthesis of enantiomeric misonidazole was performed according to the procedure developed by Jin *et al.* [12]. For the preparation of (*S*)-misonidazole (*S*)-**6**, 2-nitroimidazole (**4**) was added to commercially available (*2S*)-2-(methoxymethyl)oxirane (*S*)-**5** and sodium carbonate in dry ethanol and heated. The

crude product had to be purified by column chromatography; product-containing fractions were evaporated *in vacuo* and freeze-dried to give (*S*)-misonidazole as an orange oil. The (*R*)-enantiomer was prepared in a similar fashion by using (*2R*)-2-(methoxymethyl)oxirane (*R*)-**5**, but the crude product (*R*)-**6** had to be purified by a second column chromatography with various solvents since the first run revealed impurities and a subsequent bulb-to-bulb distillation revealed no success.

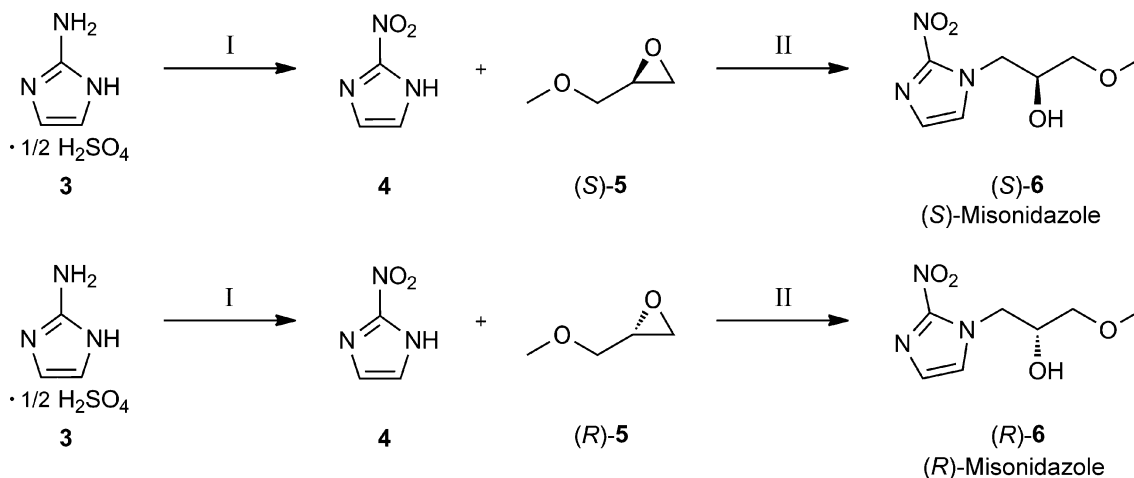
We reported a straightforward approach to synthesize the misonidazole enantiomers independently in a reasonable and practicable manner. By the combination of steps from three discrete syntheses [10–12], we obtained the chiral products from readily available chiral intermediates with overall slightly lower yields than reported. A key step was the synthesis of 2-nitroimidazole (**4**), which turned out to be accessible only in very poor yields in our hands (4%) in contrast to the reported outcome (43%) [11]. However, since the commercially available 2-nitroimidazole is very expensive, it still proved more reasonable to synthesize this intermediate from larger quantities of cheap starting material. The characterization of misonidazole enantiomers has only been incompletely described in the literature, by <sup>1</sup>H NMR and IR spectra as well as by optical rotation [12]. We hereby report on the characterization of the enantiomers of misonidazole by <sup>13</sup>C, DEPT, as well as the HSQC NMR for the (*R*)-misonidazole salt. Furthermore, high-resolution mass spectra (HRMS) and circular dichroism spectra (CDS) completed the identification and characterization of the target products. The optical rotation could not be determined by polarimetry, due to insufficient amounts of enantiomeric products, and thus had to be determined by chiral LC-UV and LC-CD.

### Identification of (+)- and (–)-enantiomers of misonidazole using chiral LC-UV and LC-CD

Since enantiomers have identical chemical and physical properties, the only way to discriminate and quantify them is by interaction with polarized light or maybe one day by nonlinear, resonant, phase-sensitive microwave spectroscopy [13]. Therefore, chiroptical high-performance liquid chromatography (HPLC) detectors to date are the logical



**Scheme 1.** Synthesis of 2-aminoimidazole hemisulfate. (I) Four hours at 50°C, then 20°C; addition of concentrated sulfuric acid. (II) Two hours stirring at 100°C.



**Scheme 2.** Synthesis of misonidazole enantiomers (I) dilute sulfuric acid, 0°C;  $\text{CuSO}_4 \cdot 5\text{H}_2\text{O}$  in water 20°C. Sodium nitrite, –10°C, –20°C gaseous  $\text{NH}_3$ . (II)  $\text{Na}_2\text{CO}_3$ , EtOH, 5 h at 60°C.

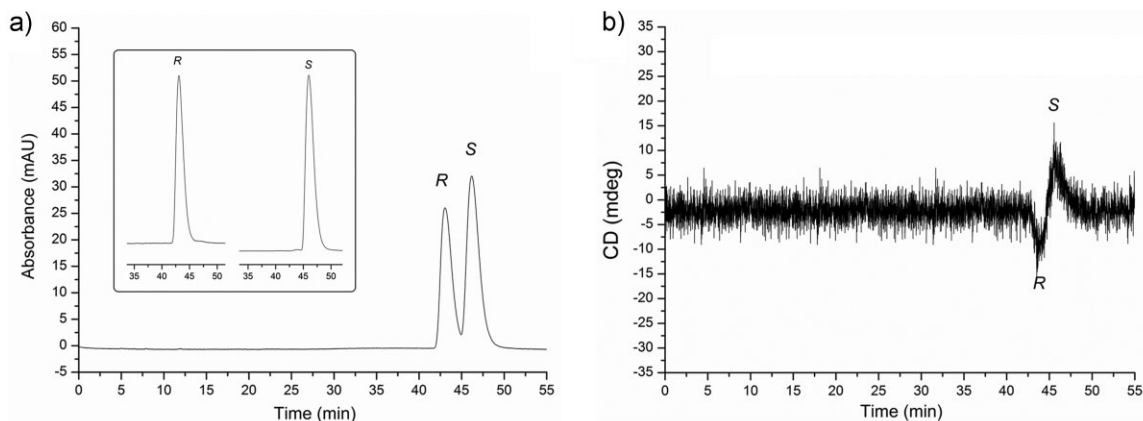
complement to any chiral separation. Circular dichroism spectroscopy is the technique of choice for determining the stereochemistry of chiral drugs and may well be used with chiral columns to verify elution order and to measure the spectra of the compounds. Selectivity and short response time also make CD an excellent detector for HPLC [14]. The influence of working wavelength, isoenantioselective temperature, and mobile phase on the output signal was recently reviewed [15]. A chiral separation method was necessary to control the enantioselective synthesis of misonidazole enantiomers. The chiral LC-UV and LC-CD separation of misonidazole enantiomers is demonstrated in Fig. 1.

Figure 2 shows the CD spectra of misonidazole enantiomers as mirror images of each other, indicating their enantiomeric nature. The CD spectra in Figs. 1 and 2 indicate *R*(–) and

*S*(+)–misonidazole, which could be assigned, since we had both analytes with known configuration in hand.

#### *In vitro* inhibition assay on bovine GPx-1

In order to determine *in vitro* inhibition of (*S*)-6, and (*R*)-6 on bovine GPx-1, an enzyme assay was used. The method has been briefly described by Kumar et al. but some details such as the exact GPX concentration were not reported. We thus optimized the method to improve the reproducibility of the literature method [9]. The assay is based on the GPX-dependent oxidation of glutathione to the disulfide (GSSG), which is recycled to GSH by glutathione reductase (GR). This step is coupled to the consumption of NADPH and the resulting decrease at  $\lambda = 340 \text{ nm}$  is monitored photometrically. We used 96-well UV-transparent microtiter plates for a



**Figure 1.** Identification of misonidazole enantiomers elution order by (a) HPLC-UV chromatogram at 295 nm for the chiral separation of the racemic mixture as well as for each enantiomer (shown in the small box). (b) HPLC-CD at 352 nm with flow cell for the LC-coupling. Chiralcel OD-H<sup>®</sup> column (5  $\mu\text{m}$ , 250 mm  $\times$  4.6 mm). Mobile phase: hexane/isopropanol 93:7 v/v at 0.6 mL/min flow rate and 40°C column temperature.

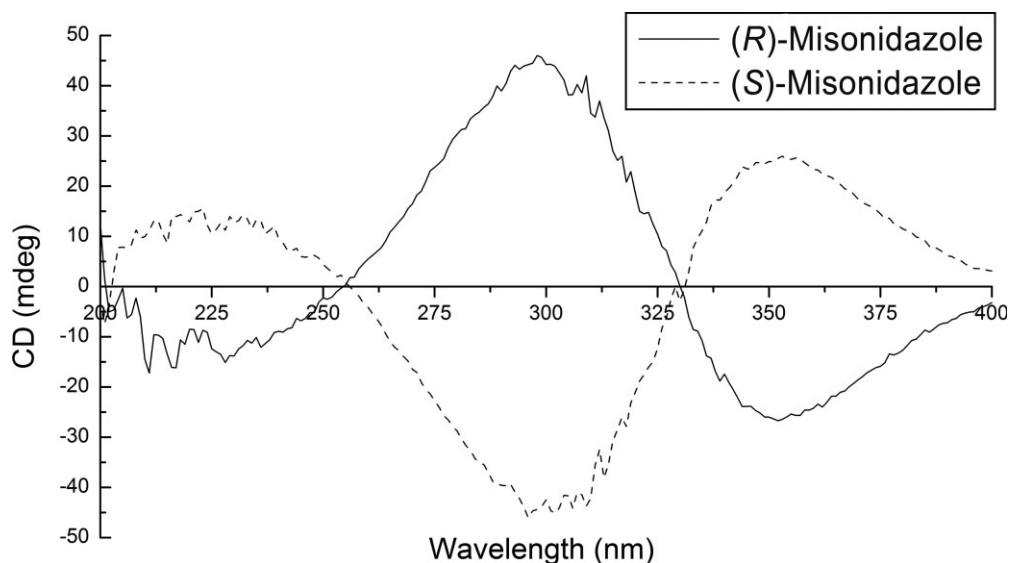


**Figure 2.** CD spectra of (*R*)- and (*S*)-misonidazole as mirror images of each other, indicating their enantiomeric nature, recorded for each enantiomer as a solution in acetonitrile (1 mg/mL) at room temperature using quartz cells (path length of 5 mm).

threefold determination of the remaining GPx-1 activity by addition of 180  $\mu\text{L}$  of tripotassium phosphate buffer (pH 7.4, 50 mM, 1.1 mM EDTA), 20  $\mu\text{L}$  of bovine erythrocyte GPx solution (0.75 IU/mL), 30  $\mu\text{L}$  of GR/NADPH mixture (baker's yeast GR solution: 2 IU/mL, NADPH solution: 2 mM), 30  $\mu\text{L}$  of inhibitor stock solution (5 mM), 30  $\mu\text{L}$  of GSH solution (2.5 mM). The addition of 30  $\mu\text{L}$   $\text{H}_2\text{O}_2$  (1 mM) started the reaction, which was measured for 12 min at intervals of 10 s at room temperature. The total volume in the microtiter plate was 300  $\mu\text{L}$  and contained 0.1% Triton X-100 to avoid precipitation of the tested compounds. The final concentrations of the used reagents were as follows: GPx 0.05 U/mL, GR 0.20 U/mL, GSH 250  $\mu\text{M}$ , NADPH 200  $\mu\text{M}$ ,  $\text{H}_2\text{O}_2$  500  $\mu\text{M}$ , misonidazole 500  $\mu\text{M}$ , and mercaptosuccinic acid 40  $\mu\text{M}$ . Mercaptosuccinic acid and misonidazole were dissolved in DMSO and hydrogen peroxide in water, respectively. All other reagents were dissolved in tripotassium phosphate buffer. The GPx-independent NADPH oxidation was controlled by the substitution of GPx solution with buffer. By replacing the inhibitor with just DMSO we determined the full enzymatic activity. The known inhibitor, mercaptosuccinic acid, served as positive control. Due to the calculation of the quotient of slopes with and without addition of the inhibitor, the remaining GPX activity was obtained.

### Biological activity

Kumar *et al.* reported that racemic misonidazole inhibits mouse GPx-1 both *in vivo* as well as *in vitro* [6]. Our findings with bovine GPx-1 show very contrary results. While the known GPX inhibitor mercaptosuccinic acid caused 83%

inhibition at 40  $\mu\text{M}$ , neither (*R*)- nor (*S*)-misonidazole, nor the racemic mixture showed significant inhibitory activity at 500  $\mu\text{M}$  (Fig. 3). (*S*)-Misonidazole free base showed extensive absorption at 340 nm, which limited the concentration that could be used in the enzyme assay. The salt formation of the (*R*)-enantiomer led to a shift of the spectral maxima, resulting in lower levels of absorption.

## Discussion

### Analysis of misonidazole enantiomers

The analysis of the final products revealed (*S*)-misonidazole as a free base, but the (*R*)-misonidazole salt, which was proved by in-depth analysis and led to slightly differing purification processes required for both enantiomers. The reason for this different behavior of the two enantiomeric products might be attributed to different qualities of the commercial samples of the two enantiomeric oxiranes (*S*)-5 and (*R*)-5. Due to the detection cutoff of the used IT-TOF mass spectrometer, the nature of the low molecular mass counter ion could not be determined. In order to ensure the identity of (*R*)-misonidazole a small aliquot was prepared as free base and the NMR signals were identical to those of the sample of (*S*)-misonidazole. The enantiomeric impurity of both products proved to be negligibly small (Fig. 1, small box).

### Suitability of misonidazole as a lead structure

In general, a good starting point for the lead optimization study is characterized by fragment-like structures with three-dimensional shape. This comprises  $\text{sp}^3$ -rich backbones with

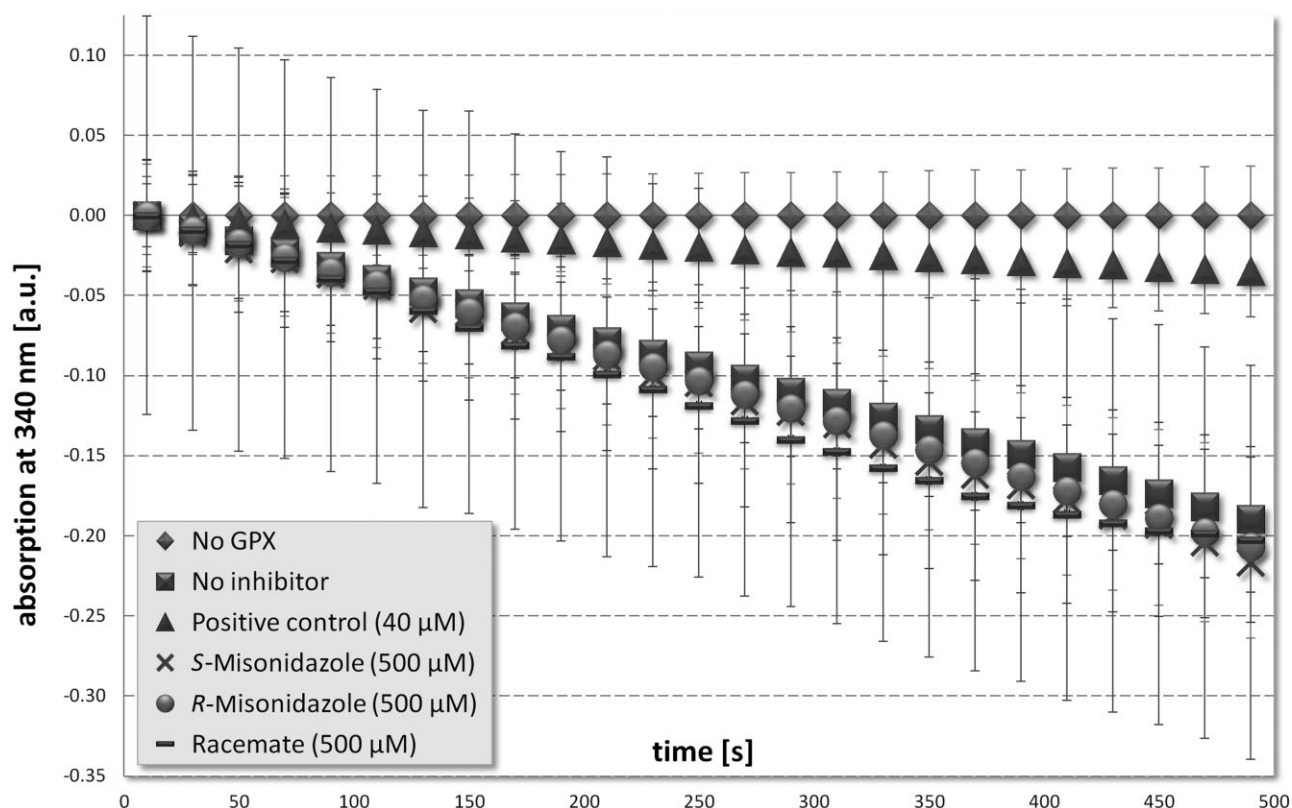


**Figure 3.** Results of the bovine GPx-1 inhibition assay: NADPH decrease over a 8-min period. Significant inhibition (lower NADPH consumption) was detected only for mercaptosuccinic acid. Due to the strong absorption of (*S*)-misonidazole free base at  $\lambda = 340$  nm the SD values are proportionally high.

defined stereochemistry and planarity disrupting structural elements, frequently present in compounds found in nature. The advantage that often comes along with such properties is a rigorous drop in crystallization tendency, which is advantageous during screening and of special importance in the later phases of galenics and pharmacokinetics. This also positively affects the water solubility, as described [16] by the general solubility equation (GSE), and thus is commonly beneficial for bioanalytical approaches. We were particularly interested in the enantiomers of misonidazole, as it meets many characteristics of a promising lead structure with tongue in cheek but still quite seriously termed as “slim and shapely” [17]. It proved to exhibit a reduced affinity for crystallization, since the melting point of racemic misonidazole was reported to be 110–111 °C [18] and both enantiomers of misonidazole were found to be semi-solid, like indicated before [12]. These low-melting properties illustrate the fact that crystal packaging of single enantiomers may differ from those of racemates considerably. In the case of the isolated (*R*)-misonidazole salt one could even speak of an ionic liquid, since the product represents a semi-solid salt under ambient conditions. Such ionic liquids are a hot topic in pharmaceu-

tical formulations due to the inherent inability to crystallize during storage of drug formulations and in the GI tract. Though our approach accordingly focused on a virtually ideal and highly promising fragment-like lead structure with “slim and shapely” design and easily exploitable synthetic diversity, the biological results restricted further efforts on the specified target enzyme.

### Evaluation of biological results

In contrast to Kumar and coworkers, we were not able to detect a significant inhibition for bovine GPx-1 at the same concentration (500  $\mu$ M). Since a racemate can show activity, while each enantiomer separately appears inactive [19], we independently screened the pure enantiomers as well as the racemic mixture on bovine GPx-1 inhibition. No effect was detected for both enantiomers, whereas the racemate showed an average inhibition of  $5.3 \pm 3.7\%$  at 500  $\mu$ M by means of threefold determination, but was not considered an effective inhibitor as well, since this activity was so low that it remains unclear whether there exists a synergistic effect between the two enantiomers. A notable difference between the two enzyme systems is the use of isolated GPx-1 from bovine

```

MCAA-----RLSAAQSTVYAFSARPLTGGEPVSLGSLRGKVLLENVASLUGGTTRDYTEMNDLQKRLGPRG    68  GPX1_MOUSE
MCAARLAA---AAAAAQSVYAFSARPLAGGEPVSLGSLRGKVLLENVASLUGGTTVRDYQMNELQRRLLGPRG    70  GPX1_HUMAN
MCAAQRSAAALAAAAPRTVYAFSARPLAGGEPFNLSLRGKVLLENVASLUGGTTVRDYQMNELQRRLLGPRG    73  GPX1_BOVIN
****:      :*** :*****.*****.*.*****.******.******.******.******
LVVLGFPCNQFGHQENGNKEEILNSLKYYRPGGGFEPNFTLFEKCEVNGEKAHPLFTFLRNALPTPSDDPTAL    141  GPX1_MOUSE
LVVLGFPCNQFGHQENAKNEEILNSLKYYRPGGGFEPNFMFLFEKCEVNGAGAHPLFAFLREALPAPSDDATAL    143  GPX1_HUMAN
LVVLGFPCNQFGHQENAKNEEILNCLKYYRPGGGFEPNFMFLFEKCEVNGEKAHPLFAFLREVLPSPDDATAL    146  GPX1_BOVIN
*****.******.******.******.******.******.******.******.******
MTDPKYIIWSPVCRNDIAWNFEKFLVGPDGVPVRRYSRRFRRTIDIEPDIETLLSQQSGNS                201  GPX1_MOUSE
MTDPKLIWSPVCRNDVAWNFEKFLVGPDGVPLRRYSRRFQTIDIEPDIETLLSQGPSCA                203  GPX1_HUMAN
MTDPKEIWSPVCRNDVSWNFEKFLVGPDGVPVRRYSRRFLTIDIEPDIETLLSQGASA-                205  GPX1_BOVIN
***** * *****.*:*****.******.******.******.******.******

```

**Figure 4.** Alignment of mouse, human, and bovine GPx-1; highlighted in gray: active site, which are all residues containing at least one atom within 4.5 Å of the catalytic tetrad atoms; highlighted in gray and underlined: non-conserved active site amino acids; framed in black: catalytic tetrad; \*, identical; :, conserved; ., semiconserved; data compiled on www.uniprot.com.

erythrocytes in our work and the use of mouse liver cytosol from post-mitochondrial supernatant fractions by Kumar *et al.* Still the enzyme activity measured by Kumar and coworkers should mainly come from the GPx-1 activity in the mouse liver cytosol, since GPx-2 [20] and GPx-3 [21] have only minor significance in mouse liver and GPx-4 does not utilize H<sub>2</sub>O<sub>2</sub> as a substrate [22]. GPx-5 to GPx-8 are oxidoreductases not found in the liver and can be ignored in this case. The homologies between the mouse, bovine, and human proteins were examined. The overall protein consensus between bovine and mouse GPx-1 was found to be 84% and at the active site still only 86%. In contrast, the bovine and human GPx-1 show overall homology of 87%, but 93% at the active site. The catalytic tetrad is completely preserved among all enzymes (Fig. 4). Especially the differences in the protein primary structure in the active site might suffice for discriminative three-dimensional orientation of mouse and bovine proteins and thus account for the presented results. Since the X-ray crystal structure of the mouse GPx-1 is not yet available, this remains speculative.

## Experimental

### Synthesis

#### General

Medium-pressure liquid chromatography was done on silica gel from Macherey-Nagel (particle size 50–100 µm, 140–270 mesh ASTM) with Buechi devices C-630, C-601, and C-660 (column length 40 cm, column diameter 3.5 cm). Melting points were determined on a hot stage microscope by Kofler PHMK 81/3035 “Boëtius” (VEB Wägetechnik Rapido) with 16-fold amplification and are uncorrected. The specified purities were determined by the 100% method of the DAD chromatogram at wavelengths as indicated. Optical rotation was determined on a manual

polarimeter P1000 from AKRÜSS Optronic. Nuclear magnetic resonance (NMR) spectra were recorded using an Avance III instrument with Ultrashield 400 (<sup>1</sup>H: 400.2 MHz, <sup>13</sup>C: 100.6 MHz) from Bruker at 25°C with tetramethylsilane (TMS) as internal standard, using ppm scale. HRMS were obtained after HPLC with a mass spectrometer (LC-IT-TOF) from Shimadzu based on a deviance tolerance limit ≤5 ppm. Infrared (IR) spectra were recorded on a Nicolet IR200 FT-IR from Thermo Electron Corporation with diamond ATR accessory. Column chromatography for the purification of (*S*)- and (*R*)-**6** was done with silica gel 60 H. *O*-Methylisourea sulfate **1** was donated by AlzChem AG, 2-aminoacetaldehyde dimethyl acetal **2** was purchased from Acros Organics, and chiral 2-(methoxymethyl)oxiranes **5** were purchased from ABCR GmbH and Co. KG. All chemicals were used without further purification. Glutathione, GR, and GPX from bovine erythrocytes were purchased from Sigma-Aldrich. NADPH was bought from Carl Roth GmbH.

#### 2-Aminoimidazole hemisulfate (**3**)

The synthesis of 2-aminoimidazole was performed according to a procedure developed by Weinmann *et al.* [10]. Thus, 0.20 mol 2-aminoacetaldehyde dimethyl acetal **2** was added under inert argon atmosphere to 0.24 mol *O*-methylisourea sulfate **1**. The reaction mixture was stirred for 4 h at 50°C, then allowed to cool at 20°C, and 2.8 mL of concentrated sulfuric acid was added to reach a pH of 2–3, upon which the reaction mixture turned brownish. The solution further darkened while it was stirred for another 2 h at 100°C. Afterwards it was cooled with ice before slowly introduced over a 12 min period into 600 mL of ice-cold ethanol. The formed suspension was stirred for an additional hour at 0°C, then filtered off, washed twice with 20 mL of ice-cold ethanol, and dried to give **3** as light brown crystals (14.3 g). Yield: 14.3 g (0.11 mol, 54%), light brown crystals, purity: 100% (at 220 nm), m.p.: 212.1–229.7°C (decomp.); <sup>1</sup>H NMR (DMSO-*d*<sub>6</sub> + TFA-*d*<sub>1</sub>) δ = 6.85, 7.45, 11.01; <sup>13</sup>C NMR (DMSO-*d*<sub>6</sub> + TFA-*d*<sub>1</sub>) δ = 113.0, 113.1, 147.1, 147.2; HRMS [*m/z*]: found 265.0717 (2 × M + H<sub>2</sub>SO<sub>4</sub> + H)<sup>+</sup>; IR (ν): 600, 1036, 1068, 1085, 1666, 3149 cm<sup>-1</sup>.

### 2-Nitroimidazole (**4**)

The synthesis of 2-nitroimidazole was based on the procedure by Yang and Goldberg [11] and started with 2.0 mol sulfuric acid in 62.5 mL of water, which was stirred and cooled to 0°C. During the slow addition of 25 mmol CuSO<sub>4</sub>·5H<sub>2</sub>O in 62.5 mL of water and 25 mmol **3** (4.1 g) in 37.5 mL of water the temperature was kept below 20°C. The resulting green solution was cooled to –20°C and stirred vigorously. During the very careful addition of 0.5 mol sodium nitrite in 112.5 mL water the temperature was kept below –10°C; brown gas evolved and the color turned into a dark blue. The reaction mixture was allowed to stand at room temperature for 1 week to give a green solution with some white precipitate. The reaction mixture was cooled to –20°C before NH<sub>3</sub> gas was initiated under the surface to titrate the solution slowly to pH 1, while the temperature was kept below –8°C. Afterwards the reaction mixture was stirred for another 3 h at 0°C. The yellow precipitate of **4** was washed twice with 10 mL of water and dried *in vacuo*. The aqueous solution was extracted six times with 100 mL of ethyl acetate and evaporated *in vacuo*. The combined product gave 2.40 g of yellow 2-nitroimidazole. Yield: 2.4 g (21.2 mmol, 4%), yellow crystals, purity: 97% (at 254 nm), m.p.: 245.1–269.7°C (decomp.); <sup>1</sup>H NMR (DMSO-*d*<sub>6</sub>) δ = 7.41, 7.44, 14.49; <sup>13</sup>C NMR (DMSO-*d*<sub>6</sub>) δ = 126.5, 146.1 (the two methine carbon atoms give only one signal, as confirmed by HSQC and HMBC spectra); HRMS [*m/z*]: found 112.0155 (M–H)<sup>–</sup>; IR (ν): 791, 1100, 1360, 1490 cm<sup>–1</sup>.

### (S)-Misonidazole ((S)-**6**)

The synthesis of (S)-misonidazole was performed according to the procedure by Jin et al. [12]. Thus, 5.5 mmol **4** was added to 10 mmol of the (2S)-2-(methoxymethyl)oxirane (S)-**5**, 2.7 mmol Na<sub>2</sub>CO<sub>3</sub>, and 17 mL of dry ethanol. The reaction mixture was heated for 5 h at 60°C, followed by further addition of 3.3 mmol of (S)-**5** and heated for another 2 h. After addition of 50 mL of water, the product was extracted with 30 mL of dichloromethane, dried over Na<sub>2</sub>SO<sub>4</sub>, and evaporated *in vacuo*. The crude product was further purified by column chromatography; product-containing fractions were evaporated *in vacuo* and freeze-dried to give an orange oil. Mobile phase for MPLC run: petroleum ether/ethyl acetate (1:3); yield: 230 mg (1.14 mmol, 43%), orange oil, purity: 97% (at 254 nm); [α]<sub>D</sub><sup>20</sup> –16.7 (c 0.3, EtOH); <sup>1</sup>H NMR (CDCl<sub>3</sub>) δ = 3.40, 3.42–3.46, 3.50–3.53, 4.17–4.20, 4.34–4.40, 4.68–4.72, 7.07, 7.21; <sup>13</sup>C NMR (CDCl<sub>3</sub>) δ = 52.8, 59.3, 68.8, 73.6, 127.6, 127.8, 144.7; HRMS [*m/z*]: found 202.0834 (M+H)<sup>+</sup>; IR (ν): 1077, 1359, 1487, 1687 cm<sup>–1</sup>.

### Salt of (R)-Misonidazole ((R)-**6**)

To prepare the salt of (R)-misonidazole 4.2 mmol **4** was added to 7.7 mmol of the (2R)-2-(methoxymethyl) oxirane (R)-**5**, 1.9 mmol Na<sub>2</sub>CO<sub>3</sub> and 22 mL dry ethanol, and subjected to reaction for 150 min at 120°C. After further addition of 3.3 mmol (R)-**5** the reaction mixture was heated for another hour at 100°C. The reaction was stopped by addition of 50 mL of water, extracted with dichloromethane, dried over Na<sub>2</sub>SO<sub>4</sub>, and concentrated *in vacuo*. The crude product was further purified by twofold column chromatography with different solvents. Mobile phase for 1. MPLC run: ethyl acetate/methanol (9:1), Mobile phase for 2. MPLC run: gradient of pure DCM over 1% MeOH in DCM to 20% MeOH in DCM; yield: 236 mg (1.17 mmol, 28%), orange oil, purity: 100% (at 254 nm); [α]<sub>D</sub><sup>20</sup> +16.7 (c 0.3, EtOH); <sup>1</sup>H NMR (CDCl<sub>3</sub>) δ = 3.43, 3.70–3.71, 3.99–4.03, 4.13–4.18, 5.28–5.34, 6.56, 6.57, 6.65, 6.66; <sup>13</sup>C NMR (CDCl<sub>3</sub>) δ = 45.2, 59.7, 72.4, 84.8, 110.6, 129.6,

159.8; HRMS [*m/z*]: found 200.0678 (M–H)<sup>–</sup>; IR (ν): 1108, 1269, 1569, 1674 cm<sup>–1</sup>

### Chiral LC-UV and LC-CD separation of misonidazole enantiomers

Circular dichroism CD (Jasco J-710 spectropolarimeter), with flow cell for the LC-coupling (LCCD-311) connected to Jasco HPLC system consisting of DG-980-50 degasser and PU-980 intelligent HPLC-pump, was employed to develop a chiral liquid chromatographic method to control the enantioselective synthesis. By using both UV and CD detectors a good selectivity between misonidazole enantiomers was achieved. CD spectra of each enantiomer were recorded as a solution in acetonitrile (1 mg/mL) at room temperature using quartz cells with path length of 5 mm, under the following conditions: scan rate (speed) 20 nm/min, bandwidth 1 nm, response 1 s, step resolution 0.5 nm, accumulation 3, and wavelength range 200–400 nm. The spectra are average computed over three instrumental scans, and the intensities are presented in terms of ellipticity values (mdeg). A Daicel 250 mm × 4.6 mm chromatographic column packed with Chiralcel OD-H<sup>®</sup> [cellulose tris(3,5-dimethyl-phenyl-carbamate)] coated on 5 μm silica gel spherical particles (Daicel, Japan) was used for the chiral chromatography of misonidazole enantiomers. The following mobile phase for the chiral separation was used: hexane/isopropanol 93:7 v/v at 0.6 mL/min flow rate and 40°C column temperature. UV detection was performed in single wavelength mode (295 nm), and circular dichroic detection was performed at 352 nm.

The authors have declared no conflict of interest.

### References

- [1] C. N. Coleman, *Oncologist* **1996**, 1, 227–231.
- [2] M. M. Poggi, C. N. Coleman, J. B. Mitchell, *Curr. Probl. Cancer* **2001**, 25, 334–411.
- [3] G. V. Martin, J. H. Caldwell, J. S. Rasey, Z. Grunbaum, M. Cerqueira, K. A. Krohn, *J. Nucl. Med.* **1989**, 30, 194–201.
- [4] S. T. Lee, A. M. Scott, *Semin. Nucl. Med.* **2007**, 37, 451–461.
- [5] T. Huang, A. C. Civelek, H. Zheng, C. K. Ng, X. Duan, J. Li, G. C. Postel, B. Shen, X. F. Li, *Am. J. Nucl. Med. Mol. Imaging* **2013**, 3, 142–153.
- [6] K. S. Kumar, J. F. Weiss, *Biochem. Pharmacol.* **1986**, 35, 3143–3146.
- [7] G. C. Mills, *J. Biol. Chem.* **1957**, 229, 189–197.
- [8] V. Gouaze, N. Andrieu-Abadie, O. Cuvillier, S. Malagarie-Cazenave, M. F. Frisach, M. E. Mirault, T. Levade, *J. Biol. Chem.* **2002**, 277, 42867–42874.
- [9] R. Schulz, T. Emmrich, H. Lemmerhirt, U. Leffler, K. Sydow, C. Hirt, T. Kiefer, A. Link, P. J. Bednarski, *Bioorg. Med. Chem. Lett.* **2012**, 22, 6712–6715.
- [10] H. Weinmann, M. Harre, K. Koenig, E. Merten, U. Tilstam, *Tetrahedron Lett.* **2002**, 43, 593–595.
- [11] C. C. Yang, I. H. Goldberg, *J. Labelled Compd. Radiopharm.* **1989**, 27, 423–434.
- [12] C. Z. Jin, H. Nagasawa, M. Shimamura, Y. Uto, S. Inayama, Y. Takeuchi, K. L. Kirk, H. Hori, *Bioorg. Med. Chem.* **2004**, 12, 4917–4927.

- [13] D. Patterson, M. Schnell, J. M. Doyle, *Nature* **2013**, 497, 475–477.
- [14] C. Bertucci, M. Pistozzi, A. De Simone, *Anal. Bioanal. Chem.* **2010**, 398, 155–166.
- [15] N. Vanthuyne, C. Roussel, *Top Curr. Chem.* **2013**, DOI: 10.1007/128\_2013\_441.
- [16] N. Jain, S. H. Yalkowsky, *J. Pharm. Sci.* **2001**, 90, 234–252.
- [17] F. Wilde, A. Link, *Expert Opin. Drug Discov.* **2013**, 8, 597–606.
- [18] F. Hoffmann, F. Hoffmann-La Roche AG, **1966**, NL6604541.
- [19] a) J. M. Batista, A. N. Batista, D. Rinaldo, W. Vilegas, D. L. Ambrosio, R. M. Cicarelli, V. S. Bolzani, M. J. Kato, L. A. Nafie, S. N. Lopez, M. Furlan, *J. Nat. Prod.* **2011**, 74, 1154–1160; b) Q. Zhang, C. Wang, *Chirality* **2013**, DOI: 10.1002/chir.22215.
- [20] F. F. Chu, J. H. Doroshov, R. S. Esworthy, *J. Biol. Chem.* **1993**, 268, 2571–2576.
- [21] W. B. Mattes, K. K. Daniels, M. Summan, Z. A. Xu, D. L. Mendrick, *Xenobiotica* **2006**, 36, 1081–1121.
- [22] F. Ursini, M. Maiorino, C. Gregolin, *Biochim. Biophys. Acta* **1985**, 839, 62–70.